

Multiresolution Representations for Piecewise-Smooth Signals on Graphs

Siheng Chen, Aarti Singh, Jelena Kovačević

Abstract—What is a mathematically rigorous way to describe the taxi-pickup distribution in Manhattan, or the profile information in online social networks? A deep understanding of representing those data not only provides insights to the data properties, but also benefits to many subsequent processing procedures, such as denoising, sampling, recovery and localization. In this paper, we model those complex and irregular data as piecewise-smooth graph signals and propose a graph dictionary to effectively represent those graph signals. We first propose the graph multiresolution analysis, which provides a principle to design good representations. We then propose a coarse-to-fine approach, which iteratively partitions a graph into two subgraphs until we reach individual nodes. This approach efficiently implements the graph multiresolution analysis and the induced graph dictionary promotes sparse representations piecewise-smooth graph signals. Finally, we validate the proposed graph dictionary on two tasks: approximation and localization. The empirical results show that the proposed graph dictionary outperforms eight other representation methods on six datasets, including traffic networks, social networks and point cloud meshes.

Index Terms—Signal processing on graphs, signal representations, graph dictionary

I. INTRODUCTION

Today’s data is being generated from a diversity of sources, all residing on complex and irregular structures; examples include profile information in social networks, stimuli in brain connectivity networks and traffic flow in city street networks [1], [2]. The need for understanding and analyzing such complex data has led to the birth of signal processing on graphs [3], [4], which generalizes classical signal processing tools to data supported on graphs; the data is the graph signal indexed by the nodes of the underlying graph.

Modeling real-world data using piecewise-smooth graph signals. In urban settings, the intersections around shopping areas will exhibit homogeneous mobility patterns and life-style behaviors, while the intersections around residential areas will exhibit different, yet still homogeneous mobility patterns and life-style behaviors. Similarly, in social networks, within a given social circle users’ profiles tend to be homogeneous, while within a different social circle they will be different, yet still homogeneous. We can model data generated from both cases as piecewise-smooth graph signals, as they capture large variations between pieces and small variations within pieces. Figure 1 illustrates how a piecewise-smooth signal model can be used to approximate the taxi-pickup distribution in Manhattan and users’ profile information on Facebook (hard thresholding is applied for better visualization).

The piecewise-smooth signal model has been intensely studied and widely used in classical signal processing, image processing and computer graphics [5], [6], [7]. Multiresolution analysis and splines are standard representation tools

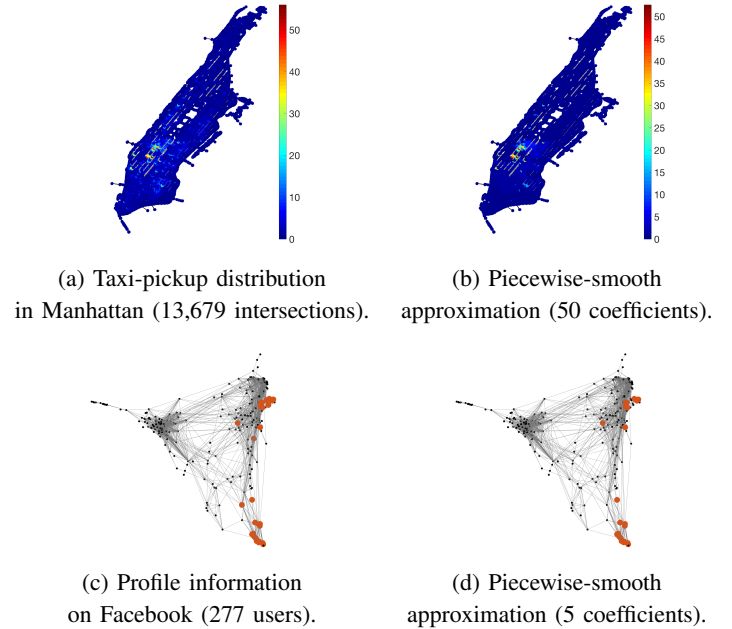


Fig. 1: Piecewise-smooth graph signals approximate irregular, nonsmooth graph signals by capturing both large variations at boundaries as well as small variations within pieces.

to analyze piecewise-smooth signals [8]. The idea of using piecewise-smooth graph signals is not novel either; in [3], the authors show that graph wavelets can capture discontinuities in a piecewise-smooth graph signal and in [9], the authors proposed denoising for piecewise-polynomial graph signals through minimizing a generalized total-variation term. There are two gaps in the previous literature we address here: (1) define piecewise-smooth graph signals precisely and find appropriate representations and (2) provide theoretical results on sparse representations for piecewise-smooth graph signals.

Representations for piecewise-smooth graph signals. Signal representations are at the heart of most signal processing techniques [10], allowing for targeted signal models for tasks such as denoising, compression, sampling, recovery and detection [11]. Our aim in this paper is to find an appropriate and efficient approach to represent piecewise-smooth graph signals.

We define a mathematical model for piecewise-smooth graph signals and propose a graph dictionary to sparsely represent piecewise-smooth graph signals. Inspired by classical signal processing, we generalize the idea of multiresolution analysis to graphs as a representation tool for piecewise-smooth signals [12]. We implement the graph multiresolution analysis by using a coarse-to-fine decomposition approach; that is,

we iteratively partition a graph into two connected subgraphs until we reach individual nodes. We show that the process leads to an efficient construction of a graph wavelet basis that satisfies the graph multiresolution analysis, and the induced graph dictionary promotes sparse representations for piecewise-smooth graph signals. We validate the proposed graph dictionaries on two tasks: approximation and localization. We show that the proposed graph dictionaries outperform eight other representation methods on six graphs, including traffic networks, citation network, social networks and point cloud meshes.

Contributions. The main contributions of this paper are:

- A novel and explicit definition for piecewise-smooth graph signals; see Section III.
- A novel graph multiresolution analysis that is implemented by a coarse-to-fine decomposition approach; see Section IV.
- A novel graph dictionary that promotes the sparsity for piecewise-smooth graph signals and is well-structured and storage-friendly; see Section III-B; and
- An extensive empirical study on a number of real-world graphs, including traffic networks, citation networks, social networks and point cloud meshes; see Section VI.

Outline of the paper. Section II reviews the background materials; Sections III defines piecewise-smooth graph signals; Section IV proposes the graph multiresolution analysis, which provides a principled way to represent graph signals. Sections III-B show that the proposed graph dictionary promotes sparse representations for piecewise-smooth graph signals. We validate the proposed methods in Section VI and conclude in Section VII.

II. BACKGROUND

We briefly introduce the framework of graph signal processing. We then overview related works on graph signal representation.

A. Graph Signal Processing

Graphs. Let $\mathcal{G} = (\mathcal{V}, \mathcal{E}, \mathbf{A})$ be an undirected, irregular and non-negative weighted graph, where $\mathcal{V} = \{v_i\}_{i=1}^N$ is the set of nodes (vertices), $\mathcal{E} = \{e_i\}_{i=1}^E$ is the set of weighted edges and $\mathbf{A} \in \mathbb{R}^{N \times N}$ is the weighted adjacency matrix whose element $A_{i,j}$ is the edge weight between the i th and the j th nodes. Let $\mathbf{D} \in \mathbb{R}^{N \times N}$ be a diagonal degree matrix with $D_{i,i} = \sum_j A_{i,j}$. The graph Laplacian matrix is $\mathbf{L} = \mathbf{D} - \mathbf{A} \in \mathbb{R}^{N \times N}$, which is a second-order difference operator on graphs [13]. Let $\Delta \in \mathbb{R}^{E \times N}$ be the graph incidence matrix; its rows correspond to edges. If e_i is an edge that connects the j th node to the k th node ($j < k$), the elements of the i th row of Δ are

$$\Delta_{i,\ell} = \begin{cases} -\sqrt{A_{j,k}}, & \ell = j; \\ \sqrt{A_{j,k}}, & \ell = k; \\ 0, & \text{otherwise.} \end{cases}$$

The graph incidence matrix measures the first-order difference and $\Delta^T \Delta = \mathbf{L}$.

Graph signals. Given a fixed ordering of nodes, we assign a signal coefficient to each node; a *graph signal* is then defined as a vector,

$$\mathbf{x} = [x_1, x_2, \dots, x_N]^T \in \mathbb{R}^N,$$

with x_n the signal coefficient corresponding to the node v_n .

We say that the graph is *smooth* when adjacent nodes have similar signal coefficients [3], [14].

- *Smoothness in the vertex domain.* Consider $\Delta \mathbf{x} \in \mathbb{R}^E$ as an *edge signal* representing the first-order difference of \mathbf{x} . The i th element of $\Delta \mathbf{x}$, $(\Delta \mathbf{x})_i = \sqrt{A_{j,k}}(x_k - x_j)$, assigns the difference between two adjacent signal coefficients to the i th edge, which connects the j th node to the k th node ($j < k$). When the variation $\|\Delta \mathbf{x}\|_2^2 = \mathbf{x}^T \mathbf{L} \mathbf{x}$ is small, the differences are small and \mathbf{x} is smooth.
- *Smoothness in the spectral domain.* We typically call this type of smoothness bandlimitedness [15], [16]. Let the graph Fourier basis $\mathbf{V} \in \mathbb{R}^{N \times N}$ be the eigenvector matrix of \mathbf{L}^1 , with $\mathbf{L} = \mathbf{V} \Lambda \mathbf{V}^T$ and the diagonal elements of Λ are arranged in ascending order. The graph spectrum is then $\hat{\mathbf{x}} = \mathbf{V}^T \mathbf{x} \in \mathbb{R}^N$. Let $\mathbf{V}_{(K)} \in \mathbb{R}^{N \times K}$ be the first K columns of \mathbf{V} , which span the lowpass bandlimited subspace. For $K \ll N$, when $\|\mathbf{V}_{(K)}^T \mathbf{x}\|_2^2 / \|\mathbf{x}\|_2^2 = 1$, the energy concentrates in the lowpass band and \mathbf{x} is smooth.

In practice, graph signals may not satisfy the smoothness constraint as above (as shown in Figure 1), which serves as motivation to further develop graph signal models and tools to represent them, the topic of this paper.

B. Related Works

Ideally, a good representation should be efficient, have some structure such as orthogonality and promote sparse representations for graph signals (at least in some subspaces). To deal with large-scale graphs, we may also need the representation itself to be sparse and storage-friendly. We categorize the previous work on graph signal representations as follows:²

1) *Graph Filter Banks:* Here, representations are constructed by generalizing classical filter banks to graphs. [17], [18] designs critically-sampled filter banks via bipartite sub-graph decomposition; [19], [20] design critically-sampled filter banks for circulant graphs; [21] designs oversampled filter banks; [22] designs iterative filter banks; [23] designs critically-sampled filter banks via community detection; and [24] designs each channel via sampling and recovery.

2) *Graph Vertex-Domain Designs:* Here, representations are constructed by designing each basis vector (atom) in the graph vertex domain. [25] designs spatial wavelets via neighborhoods; and [26], [27], [28], [29] considers coarse-to-fine approaches.

3) *Graph Spectral-Domain Designs:* Here, representations are constructed by designing graph filters in the graph spectral domain. [30] designs graph wavelets; [31], [32] design tight frames; and [33] designs the windowed graph Fourier transforms by generalizing translation.

¹The graph Fourier basis can also be defined based on adjacency matrix [4].

²The categorization follows from https://www.macalester.edu/~dshuman1/Talks/Shuman_GSP_2016.pdf.

4) *Graph Diffusion-Based Designs*: Here, representations are constructed based on the polynomial of the transition matrix. [34] designs diffusion wavelets; and [35] designs diffusion wavelet packets;

5) *Graph Dictionary Learning*: Here, representations are constructed by learning from the given graph signals. The representations in the other branches depend on the graph structure only; [36], [37] learn graph dictionaries that provide smoothness for given graph signals, which is adaptive and biased to the observed graph signals.

In this paper, we consider connecting graph filter banks and graph vertex domain designs. Similarly to [26], [27], [28], [29], [23], the proposed representation considers the coarse-to-fine decomposition in the graph vertex domain. Our goal is to implement the graph multiresolution analysis, where the coarse-to-fine approach is more efficient and straightforward than the local-to-global approach (graph filter banks). We further show that the proposed representation is efficient, orthogonal and storage-friendly; it also satisfies the graph multiresolution analysis and promotes the sparsity for piecewise-constant and piecewise-smooth graph signals.

The representations of smooth graph signals have been thoroughly studied in the graph spectral domain [38], [39]. In this paper, we emphasize the representations of piecewise-smooth graph signals in the graph vertex domain. As a continuous counterpart of graph signal representations, some other works study on manifold data representations [40], [41], [42].

III. GRAPH SIGNAL MODELS

Piecewise-smooth graph signals can model a number of real-world cases as they capture large variations between pieces and small variations within pieces. In this section, we mathematically define piecewise-smooth graph signals. We start with piecewise-constant graph signals, an important subclass, and then extend it to piecewise-smooth graph signals.

A. Piecewise-Constant Model

In classical signal processing, a piecewise-constant signal is a signal that is locally constant over connected regions separated by lower-dimensional boundaries. Such a signal is often related to step functions, square waves and Haar wavelets and is widely used in image processing [10]. Piecewise-constant graph signals have been used in many applications without having been explicitly defined; for example, in community detection, community labels form a piecewise-constant graph signal for a given social network and in semi-supervised learning, classification labels form a piecewise-constant graph signal for a graph constructed from the dataset. While smooth graph signals emphasize slow transitions, piecewise-constant graph signals emphasize fast transitions (corresponding to boundaries) and localization in the vertex domain (corresponding to signals being nonzero in a local neighborhood).

We define a piecewise-constant graph signal through the concept of a piece that has been implicitly used before [43], [44]. The definition is intuitive; a piecewise-constant graph signal partitions a graph into several pieces; within each piece, signal coefficients are constant.

Definition 1. Let S be a subset of the node set \mathcal{V} . We call S a *piece* when its corresponding subgraph G_S is connected.

We can represent a piece S by using a one-piece graph signal, $\mathbf{1}_S \in \mathbb{R}^N$. A piecewise-constant graph signal is a linear combination of several one-piece graph signals.

Definition 2. Let $\{S_c\}_{c=1}^C$ be a partition of the node set \mathcal{V} , where each S_c is a piece. A graph signal $\mathbf{x} \in \mathbb{R}^N$ is piecewise-constant with C pieces when

$$\mathbf{x} = \sum_{c=1}^C a_c \mathbf{1}_{S_c},$$

where $a_c \in \mathbb{R}$ is the piece coefficient for the piece S_c . Denote this class by $\text{PC}(C)$.

For most graph signals, two adjacent signal coefficients are typically the same; that is, $\|\Delta\mathbf{x}\|_0$ may be close to the number of edges E . For a piecewise-constant graph signal \mathbf{x} with a few number of pieces, however, $\|\Delta\mathbf{x}\|_0$ is usually small. Within a piece, it is 0 while across pieces, $\|\Delta\mathbf{x}\|_0$ is the cut cost to separate the pieces. For example, in an unweighted graph,

$$\|\Delta\mathbf{x}\|_0 \leq \# \text{ edges across pieces } \{S_c\}_{c=1}^C,$$

for all $\mathbf{x} \in \text{PC}(C)$, where the equality is achieved when all a_c are different. Thus, $\|\Delta\mathbf{x}\|_0 \ll E$ when $C \ll N$; see a quick summary in Table I.

Graph signal models	Properties	
	$\ \Delta\mathbf{x}\ _0$	$\ \Delta\mathbf{x}\ _2$
Arbitrary graph signal	$O(E)$	large
Smooth graph signal	$O(E)$	small
Piecewise-constant graph signal	$O(1)$	large

TABLE I: Property summary of some typical graph signals.

B. Piecewise-Smooth Model

Piecewise-smooth signals are widely used to represent images, where edges are captured by the piece boundaries and smooth content is captured by the pieces themselves. Piecewise-smooth graph signals arise naturally from piecewise-constant graph signals with more flexibility to model real-world data, such as taxi-pickup distribution supported on the city-street networks and 3D point cloud information supported on the meshes.

We define a piecewise-smooth graph signal as a generalization of a piecewise-constant graph signal. For a piecewise-constant signal, signal coefficients within a piece are constant; for a piecewise-smooth signal, signal coefficients within a piece form a smooth graph signal over that piece.

Let S be a piece, G_S be the corresponding subgraph, $\mathbf{V}_S \in \mathbb{R}^{|S| \times |S|}$ be the corresponding graph Fourier basis. Given a graph signal $\mathbf{x} \in \mathbb{R}^N$, $\mathbf{x}_S \in \mathbb{R}^{|S|}$ denotes the signal coefficients supported on G_S and $\mathbf{x}_{\bar{S}} \in \mathbb{R}^{N-|S|}$ denotes the rest signal coefficients.

Definition 3. A graph signal $\mathbf{x} \in \mathbb{R}^N$ is localized and bandlimited over the piece S with bandwidth K ($K \leq |S|$) when $\mathbf{x}_{\bar{S}} = \mathbf{0}$ and

$$\mathbf{V}_{S(K)} \mathbf{V}_{S(K)}^T \mathbf{x}_S = \mathbf{x}_S \in \mathbb{R}^{|S|},$$

where $V_{S(K)} \in \mathbb{R}^{|S| \times K}$ contains the first K columns of the graph Fourier basis V_S .

Definition 3 shows a class of graph signals that is localized in both the vertex and the graph spectral domains. Since these signals are bandlimited over a piece, we consider them lowpass and smooth within this piece. A similar definition has also been proposed in [45]; the difference is that the bandlimitedness in [45] is defined for the entire graph, while the bandlimitedness in Definition 3 is defined for a subgraph only. We then consider piecewise-bandlimited graph signals as a linear combination of localized and bandlimited graph signals.

Definition 4. A graph signal $\mathbf{x} \in \mathbb{R}^N$ is piecewise-bandlimited with C pieces and bandwidth K when $\mathbf{x} = \sum_{c=1}^C \mathbf{x}^{(c,K)}$, where each $\{S_c\}$, $c = 1, \dots, C$ is a valid piece and $\mathbf{x}^{(c,K)} \in \mathbb{R}^N$ is bandlimited over the piece S_c with bandwidth K . Denote this class by $\text{PBL}(C, K)$.

IV. GRAPH MULTIREOLUTION

Having defined a piecewise-smooth model for the data we are interested in, we now embark upon looking for the appropriate representations. Inspired by classical signal processing, we generalize the multiresolution analysis to graph signals and propose a coarse-to-fine approach to implement it.

A. Graph Multiresolution Analysis

Definition 5. A multiresolution analysis on graphs consists of a sequence of embedded closed subspaces $V^{(L)} \subset \dots \subset V^{(1)} \subset V^{(0)}$, such that

- it satisfies upward completeness, $V^{(0)} = \mathbb{R}^N$;
- it satisfies downward completeness, $V^{(L)} = \{c\mathbf{1}_V, c \in \mathbb{R}\}$;
- there exists an orthonormal basis $\{\mathbf{v}_k^{(\ell)}\}_{k=0}^{K^{(\ell)}-1}$ for $V^{(\ell)}$;
- it satisfies generalized shift invariance, that is, for any $\mathbf{x} \in V^{(\ell)}$, there exists a nontrivial permutation operator $\Phi \in \{0, 1\}^{N \times N}$ ($\Phi \mathbf{1} = \Phi^T \mathbf{1} = \mathbf{1}$) such that $\Phi \mathbf{x} \in V^{(\ell)}$. The permutation operator Φ only allows for swapping signal coefficients in two nonoverlapping pieces.
- it satisfies generalized scale invariance; that is, for any $\mathbf{x} \in V^{(\ell)}$, there exists a nontrivial permutation operator, $\Phi \in \{0, 1\}^{N \times N}$ such that $\Phi \mathbf{x} \in V^{(\ell)}$. When the permutation operator Φ swaps signal coefficients in two nonoverlapping pieces, each piece has at most 2^ℓ nodes.

While similar in spirit, the proposed graph multiresolution analysis is different from the original one [12]. For example, the complete space here is \mathbb{R}^N instead of $\mathcal{L}_2(\mathbb{R})$ because of the discrete nature of the graph. We unify the shift and scale invariance axioms via a permutation operator, which reshapes a graph signal by swapping signal coefficients. The standard shift invariance axiom ensures that the input signal shape is preserved during shifting; here, this is accomplished by requiring that the permutation operator swap the signal coefficients supported on two nonoverlapping pieces only. The standard scale invariance axiom ensures that the input signal shape is preserved during scaling; here, this is accomplished by requiring that the number of swaps scale exponentially as the multiresolution level ℓ grows; see Figure 3 for illustration.

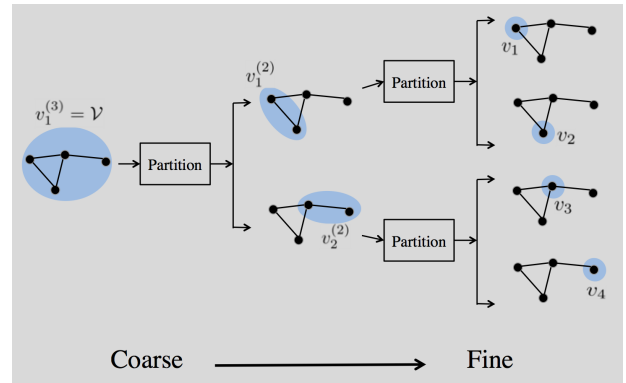
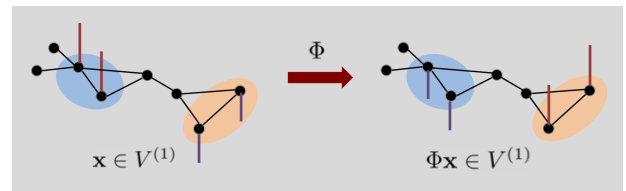
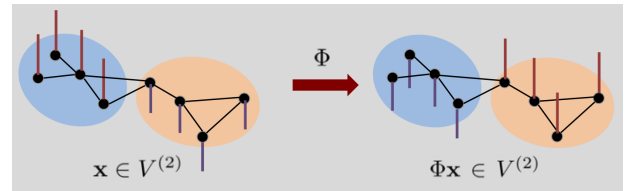


Fig. 2: Coarse-to-fine decomposition approach. At each step, we partition a larger piece into two smaller disjoint pieces and generate a pair of lowpass/highpass basis vectors. Piece $v_1^{(3)} = \mathcal{V}$ is at Level 3; Pieces $v_1^{(2)}, v_2^{(2)}$ are at Level 2; and Pieces v_1, v_2, v_3, v_4 are at Level 1.



(a) Permutation in $V^{(1)}$. We swap the signal coefficients between the blue piece and the yellow piece. The total number of swaps is 2.



(b) Permutation in $V^{(2)}$. We swap the signal coefficients between the blue piece and the yellow piece. The total number of swaps is 4.

Fig. 3: Permutation leads to the generalized shift and scale invariances. The permutation operator Φ shifts a graph signal $\mathbf{x} \in V^{(\ell)}$ to another graph signal $\Phi \mathbf{x} \in V^{(\ell)}$ by swapping signal coefficients supported on two difference pieces, which leads to the generalized shift invariance; the permutation operator needs twice as many swaps to permute a graph signal in a coarser space, which leads to the generalized scale invariance.

B. Coarse-to-Fine Construction

Our goal now is to implement the graph multiresolution analysis. In classical signal processing, this is typically accomplished by using filter banks, which involves a series of downsampling and shifting. Filter banks start with building filters in a fine space, which captures local information, and gradually building them in coarser spaces, which captures global information. For discrete-time signals, filter banks happen to be an efficient way to implement the multiresolution analysis because the downsampling and shifting operators follow naturally. For graph signals, however, there is no recipe to permute the nodes; thus, it is hard to obtain efficient downsampling and shifting

operators; see details in Appendix A.

Instead, we consider implementing graph multiresolution analysis using a *coarse-to-fine approach*. The main idea is to recursively partition each piece into two smaller disjoint child pieces as follows: Given a connected graph $G_0(\mathcal{V}_0, \mathcal{E}_0, A_0)$ with $|\mathcal{V}_0| > 1$, partition G_0 into two smaller graphs $G_1(\mathcal{V}_1, \mathcal{E}_1, A_1)$ and $G_2(\mathcal{V}_2, \mathcal{E}_2, A_2)$ by solving

$$\min_{\mathcal{V}_1, \mathcal{V}_2} \quad \left| |\mathcal{V}_1| - |\mathcal{V}_2| \right| \quad (1a)$$

$$\text{subject to} \quad \mathcal{V}_1 \cap \mathcal{V}_2 = \emptyset, \mathcal{V}_1 \cup \mathcal{V}_2 = \mathcal{V}_0, \quad (1b)$$

$$G_1, G_2 \text{ are connected.}$$

In other words, we want (1) each of the two child pieces to be connected; and (2) the partition to be close to a bisection; that is, the difference between cardinalities of two child pieces is as small as possible. These properties ensure that the coarse-to-fine approach implements the graph multiresolution analysis. We solve (1) in Section IV-D.

We start with the coarsest lowpass subspace $V^{(0)} = \{c\mathbf{1}_{\mathcal{V}}, c \in \mathbb{R}\}$ and partition the largest piece \mathcal{V} into two disjoint and connected child pieces $v_1^{(1)}, v_2^{(1)} \subseteq \mathcal{V}$; that is, $v_1^{(1)} \cup v_2^{(1)} = \mathcal{V}, v_1^{(1)} \cap v_2^{(1)} = \emptyset$, where the subscript denotes the index at each level. The lowpass/highpass basis vectors are, respectively,

$$\mathbf{v}_1^{(1)} = g(v_1^{(1)}, v_2^{(1)}),$$

$$\mathbf{u}_1^{(1)} = h(v_1^{(1)}, v_2^{(1)}),$$

where

$$g(S_1, S_2) = \sqrt{\frac{|S_1||S_2|}{|S_1|+|S_2|}} \left(\frac{\mathbf{1}_{S_1}}{|S_1|} + \frac{\mathbf{1}_{S_2}}{|S_2|} \right) \in \mathbb{R}^N,$$

$$h(S_1, S_2) = \sqrt{\frac{|S_1||S_2|}{|S_1|+|S_2|}} \left(\frac{\mathbf{1}_{S_1}}{|S_1|} - \frac{\mathbf{1}_{S_2}}{|S_2|} \right) \in \mathbb{R}^N,$$

with $S_1, S_2 \subset \mathcal{V}$ two nonoverlapping pieces. The normalization ensures that each basis vector is of unit norm and $\mathbf{1}^T \mathbf{u}_1^{(1)} = 1$. The highpass subspace is $U^{(1)} = \{c\mathbf{u}_1^{(1)}, c \in \mathbb{R}\}$.

We now partition pieces $v_1^{(1)}$ and $v_2^{(1)}$ to obtain $v_1^{(2)}, v_2^{(2)}$ and $v_3^{(2)}, v_4^{(2)}$, respectively. The lowpass/highpass basis vectors are

$$\mathbf{v}_k^{(2)} = g(v_{2k-1}^{(2)}, v_{2k}^{(2)}),$$

$$\mathbf{u}_k^{(2)} = h(v_{2k-1}^{(2)}, v_{2k}^{(2)}),$$

for $k = 1, 2$. The lowpass subspace is $V^{(2)} = \text{span} \left(\left\{ \mathbf{v}_k^{(2)} \right\}_{k=1}^{K^{(2)}} \right)$ and the highpass subspace is $U^{(2)} = \text{span} \left(\left\{ \mathbf{u}_k^{(2)} \right\}_{k=1}^{K^{(2)}} \right)$, where $K^{(2)} = 2$. We keep on partitioning, building the lowpass and highpass subspaces and their corresponding bases in the process.

At the ℓ th level, we partition $v_k^{(\ell+1)}$ to obtain $v_{2k-1}^{(\ell)}, v_{2k}^{(\ell)}$. When both $v_{2k-1}^{(\ell)}, v_{2k}^{(\ell)}$ are nonempty,

$$\mathbf{v}_k^{(\ell)} = g(v_{2k-1}^{(\ell)}, v_{2k}^{(\ell)})$$

is a lowpass basis vector and

$$\mathbf{u}_k^{(\ell)} = h(v_{2k-1}^{(\ell)}, v_{2k}^{(\ell)})$$

is a highpass basis vector; when one of them is empty, the cardinality of $v_k^{(\ell+1)}$ is 1 and we cease partitioning in this branch. At the finest resolution, each piece corresponds to an individual node. Since we promote bisection, the total decomposition depth L is around $1 + \log_2 N$.

At the end of the process, we collect all highpass basis vectors into a Haar-like graph wavelet basis (see Algorithm 1). A toy example is shown in Figure 2.

Algorithm 1 Haar-like Graph Wavelet Basis Construction

Input $G(\mathcal{V}, \mathcal{E}, A)$ graph
Output W wavelet basis

Function

- 1) initialize a stack of pieces sets \mathbb{S} and a set of vectors W
 - 2) push $S = \mathcal{V}$ into \mathbb{S}
 - 3) add $\mathbf{w} = \frac{1}{\sqrt{|S|}} \mathbf{1}_S$ to W
 - 4) while the cardinality of the largest element in \mathbb{S} is larger than 1
 - 4.1) pop up one element from \mathbb{S} as S
 - 4.2) evenly partition S into two disjoint pieces S_1, S_2
 - 4.3) push S_1, S_2 into \mathbb{S}
 - 4.4) add $\mathbf{w} = \sqrt{\frac{|S_1||S_2|}{|S_1|+|S_2|}} \left(\frac{1}{|S_1|} \mathbf{1}_{S_1} - \frac{1}{|S_2|} \mathbf{1}_{S_2} \right)$ to W
- return** W
-

C. Graph Wavelet Basis Properties

1) *Efficiency*: This coarse-to-fine approach involves $(N-1)$ partitions. The overall computational complexity is approximately $\sum_{\ell=1}^{1+\log_2 N} 2^\ell f(N/2^\ell)$, where $f(N)$ is the computational complexity of partitioning an N -node graph. For a sparse graph ($E = O(N)$), when we use a standard graph partitioning algorithm, METIS [46], to partition the graph, $f(N) = O(N)$ and the overall computational complexity is $O(N \log_2 N)$.

2) *Graph multiresolution*: When the number of nodes $N = 2^L$ for some $L \in \mathbb{Z}_+$, the proposed graph wavelet basis in Algorithm 1 satisfies the axioms of the graph multiresolution analysis. When the number of nodes cannot be partitioned equally, the proposed graph wavelet basis may not exactly satisfy the generalized shift and scale invariance axioms due to the residual condition, but still comes close to the spirit of multiresolution.

3) *Orthogonality*: Orthogonality also implies efficient perfect reconstruction.

Theorem 1. The proposed graph wavelet basis $W \in \mathbb{R}^{N \times N}$ in Algorithm 1 is orthonormal; that is, for any graph signal $\mathbf{x} \in \mathbb{R}$, we have $\mathbf{x} = W W^T \mathbf{x}$.

The proof is given in Appendix B.

D. Graph Partition Algorithm

An ideal graph partitioning results in two connected subgraphs with the same number of nodes; however, connectivity and bisection may conflict in practice. Many existing graph partition algorithms can be used in graph partition. For example, METIS provides an efficient bisection, but does not ensure that two resulting subgraphs are connected. In (1), we consider the connectivity-first approach, as the constraints (1b) requires that the resulting subgraphs be connected. The objective function (1a) promotes a bisection; that is, two subgraphs

have similar number of nodes. The optimization problem (1) is combinatorial and we aim to obtain a suboptimal solution with certain theoretical guarantee.

To solve (1), we consider finding two nodes with the longest geodesic distance as two hubs and then compute the geodesic distances from each nodes to two hubs. We rank all the nodes based on the difference between the geodesic distances to two hubs and record the median value. We partition the nodes according to this median value. All the nodes falling into the median value forms the boundary set. We further partition the boundary set to ensure connectivity and promote bisection. The details are summarized in Algorithm 2.

Algorithm 2 Graph Partition with Connectivity Guarantee

Input G_0 original graph
Output $\mathcal{V}_1, \mathcal{V}_2$ two node sets

Function

- 1) compute the geodesic distance matrix $D \in \mathbb{R}^{|\mathcal{V}_0| \times |\mathcal{V}_0|}$;
 - 2) select $v_i, v_j \in \mathcal{V}_0$, such that D_{v_i, v_j} is maximized;
 - 3) let p be median value of $D_{v_i, \cdot} - D_{v_j, \cdot}$;
 - 4) let $S_1 = \{v | D_{v_i, v} - D_{v_j, v} > p\}$ and boundary set $S_2 = \{v | D_{v_i, v} - D_{v_j, v} = p\}$;
 - 5) partition S_2 into connected components C_1, C_2, \dots, C_M with $|C_1| < |C_2| < \dots < |C_M|$.
 - 6) set $q_m = |S_1 \cup C_1 \cup \dots \cup C_m|$ for $m = 1, 2, \dots, M$;
 - 7) set $m^* = \arg \min_m |q_m - |\mathcal{V}_0|/2|$;
 - 8) $\mathcal{V}_1 = S_1 \cup C_1 \cup \dots \cup C_{m^*}$ and $\mathcal{V}_2 = \mathcal{V}_0 \setminus \mathcal{V}_1$
- end
return $\mathcal{V}_1, \mathcal{V}_2$
-

We can show that Algorithm 2 provides a near-optimal solution; see Appendix C for the proof.

Theorem 2. Let $\widehat{\mathcal{V}}_1, \widehat{\mathcal{V}}_2$ be the solution given by Algorithm 2. Then, $\widehat{\mathcal{V}}_1, \widehat{\mathcal{V}}_2$ is a feasible solution of the optimization problem (1) and

$$||\widehat{\mathcal{V}}_1| - |\widehat{\mathcal{V}}_2|| \leq 2|C_{m^*}|,$$

where C_{m^*} is the m^* th smallest connected component in the boundary set, following from the Steps 5-7 in Algorithm 2.

V. GRAPH DICTIONARIES

We now use the graph dictionary induced by the graph multiresolution analysis from the previous section to represent piecewise-smooth graph signals. As before, we start with piecewise-constant graph signals and then generalize to the piecewise-smooth ones.

A. Piecewise-Constant Graph Dictionary

Representing piecewise-constant graph signals is difficult because the geometry of the pieces is arbitrary. We now show that the graph wavelet basis in Algorithm 1 can effectively parse the pieces and promote the sparse representations for piecewise-constant graph signals.

Theorem 3. Let $W \in \mathbb{R}^{N \times N}$ be the graph wavelet basis in Algorithm 1. For a piecewise-constant graph signal $\mathbf{x} \in \mathbb{R}^N$,

$$\|W^T \mathbf{x}\|_0 \leq 1 + \|\Delta \mathbf{x}\|_0 L,$$

where L is the decomposition depth.

The proof is given in Appendix D. Since we promote the bisection scheme, L is roughly $1 + \log_2 N$. Theorem 3 shows an upper bound on the sparsity of graph wavelet coefficients, which depends on the cut cost $\|\Delta \mathbf{x}\|_0$ and the size of the graph. As shown in Table I, $\|\Delta \mathbf{x}\|_0$ is usually small when \mathbf{x} is a piecewise-constant signal. In [47], we also show that this graph wavelet basis can be used to detect localized graph signals.

We can expand the graph wavelet basis from Algorithm 1 to a redundant graph dictionary, allowing for more flexibility. Each piece $v_k^{(\ell)}$ obtained from the graph partition is a column vector (called an atom) $\mathbf{1}_{v_k^{(\ell)}}$ in the graph dictionary; we collect all the pieces at all levels to obtain a dictionary. In other words, the *piecewise-constant graph dictionary* is

$$D_{\text{PC}} = \{\mathbf{1}_{v_k^{(\ell)}}\}_{\ell=1, k=1}^{\ell=L, k=2^\ell}. \quad (2)$$

There are $2N - 1$ pieces in total; thus, $D_{\text{PC}} \in \mathbb{R}^{N \times (2N-1)}$ and the proposed graph dictionary D_{PC} contains a series of atoms with different sizes activating different positions. Each graph wavelet basis vector in Algorithm 1 can be represented as a linear combination of two atoms in the piecewise-constant graph dictionary.

Since most atoms are sparse, the number of nonzero elements in the piecewise-constant dictionary is small, allowing for efficient storage. For example, when $N = 2^L$ for some $L = \mathbb{Z}_+$, the number of nonzero elements is exactly NL .

Corollary 1. Let $D_{\text{PC}} \in \mathbb{R}^{N \times (2N-1)}$ be the piecewise-constant graph dictionary. Let the sparse coefficients of a piecewise-constant graph signal $\mathbf{x} \in \text{PC}(C)$ be

$$\mathbf{a}^* = \arg \min_{\mathbf{a} \in \mathbb{R}^{2N-1}} \|\mathbf{a}\|_0, \quad (3)$$

subject to $\mathbf{x} = D_{\text{PC}} \mathbf{a}$.

Then, we have

$$\|\mathbf{a}^*\|_0 \leq 1 + \|\Delta \mathbf{x}\|_0 L.$$

Corollary 1 directly follows from Theorem 3, as the graph wavelet basis can be linearly represented by the piecewise-constant graph dictionary. We expect the upper bound in Corollary 1 is not tight. In practice, the corresponding sparsity is usually even smaller than the sparsity provided by the graph wavelet basis because of the redundancy and flexibility of the piecewise-constant graph dictionary.

B. Piecewise-Smooth Graph Dictionary

We now generalize the piecewise-constant graph dictionary to the piecewise-smooth graph dictionary. In the piecewise-constant graph dictionary, we use a single one-piece graph signal to activate a certain subgraph; in the piecewise-smooth graph dictionary, we can use multiple localized and bandlimited graph signals to activate the same subgraph. Since localized and bandlimited graph signals are smooth on the corresponding subgraphs, the piecewise-smooth graph dictionary provides more redundancy and flexibility to capture the localized events within a graph signal.

Let v_k^ℓ be the k th piece in the ℓ th decomposition level, $G_{v_k^\ell}$ the corresponding subgraph and $V_{v_k^\ell} \in \mathbb{R}^{|\mathcal{V}_k^\ell| \times |\mathcal{V}_k^\ell|}$ the corresponding graph Fourier basis. The subdictionary corresponding

to the k th piece at the ℓ th decomposition level is

$$D_{v_k^\ell} = V_{v_k^\ell(K)} \in \mathbb{R}^{|v_k^\ell| \times \min(K, |v_k^\ell|)},$$

which is the first $\min(K, |v_k^\ell|)$ columns of $V_{v_k^\ell}$. We collect all subdictionaries across all levels to obtain the *piecewise-smooth graph dictionary*,

$$D_{\text{PS}} = \{D_{v_k^\ell}\}_{\ell=1, k=1}^{\ell=L, k=2^\ell}. \quad (4)$$

The total number of atoms of D_{PS} is upper bounded by $(2N - 1)K$ with bandwidth K . The total number of nonzero elements of D_{PS} is at most $O(NK \log_2 N)$, still storage friendly.

We now show that D_{PS} promotes sparsity for piecewise-bandlimited graph signals.

Theorem 4. Let D_{PS} be the piecewise-smooth graph dictionary. Let the sparse coefficient of a piecewise-bandlimited graph signal $x \in \text{PBL}(C, K)$ be

$$\begin{aligned} \mathbf{a}^* &= \arg \min_{\mathbf{a}} \|\mathbf{a}\|_0, \\ &\text{subject to } \|\mathbf{x} - D_{\text{PS}} \mathbf{a}\|_2^2 \leq \epsilon_{\text{par}} \|\mathbf{x}\|_2^2, \end{aligned}$$

where ϵ_{par} is a constant determined by the graph partitioning algorithm. Then, we have

$$\|\mathbf{a}^*\|_0 \leq 1 + 2K \|\Delta \mathbf{x}_{\text{PC}}\|_0 L,$$

where L is the decomposition depth in the coarse-to-fine approach and \mathbf{x}_{PC} is a piecewise-constant signal that shares the same pieces with \mathbf{x} .

The proof is given in Appendix E.

VI. EXPERIMENTAL RESULTS

A good representation can be used in compression, approximation, inpainting, denoising and localization. Here we evaluate our proposed graph dictionaries on two tasks: approximation and localization.

A. Experimental Setup

We consider six datasets summarized in Table II.

- **Sensors.** This is a simulated geometric graph with 500 nodes and 2,050 edges. We simulate a piecewise-smooth graph signal following [22].
- **Minnesota.** This is the Minnesota road network with 2,642 intersections and 3,304 road segments. We model each intersection as a node and each road segment as an edge. We simulate a localized smooth graph signal following [22].
- **Manhattan.** This is the Manhattan street network with 13,679 intersections and 34,326 road segments. We model each intersection as a node and each road segment as an edge. We model the restaurant distribution, and taxi-pickup positions as signals supported on the Manhattan street network.
- **Kaggle 1968.** This is a social network of Facebook users with 277 nodes and 2,321 edges. It also contains 14 social circles, where each one can be modeled as a binary piecewise-constant signal supported on this social network.

- **Citeseer.** This is a co-authorship network with 2,120 nodes and 3,705 edges. It also contains 7 research groups, where each one can be modeled as a binary piecewise-constant signal supported on this co-authorship network.
- **Teapot.** This is a dataset with 7,999 3D points, representing the surface of a teapot. We construct a 10-nearest neighbor graph to capture the geometry. 3D coordinates can be modeled as three piecewise-smooth signals supported on this generalized mesh.

Dataset	Type	# nodes	# edges	Signals
Sensors	Simulation	500	2,050	Simulation
Minnesota	Traffic net	2,642	3,304	Simulation
Manhattan	Traffic net	13,679	3,679	Taxi
Kaggle 1968	Social net	277	2,321	Circle
Citeseer	Citation net	2,120	3,705	Attribute
Teapot	Mesh	7,999	198,035	Coordinate

TABLE II: Dataset description.

We consider the following ten competitive representation methods:

- **PC** (dashed dark red line). This is our piecewise-constant graph dictionary (2).
- **PS** (solid red line). This is our piecewise-smooth graph dictionary (4). The bandwidth in each piece is 10.
- **Delta** (solid dark yellow line). This is the basis of Kronecker deltas.
- **GFT** (dashed yellow line) [3]. This is the graph Fourier basis.
- **SGWT** (solid blue line) [30]. This is the spectral graph wavelet transform with five wavelet scales plus the scaling functions for a total redundancy of 6.
- **Pyramid** (dashed light blue line) [22]. This is the multi-scale pyramid transform.
- **CKWT** (solid grey line) [25]. These are spatial graph wavelets with wavelet functions based on the renormalized one-sided Mexican hat wavelet, also with five wavelet scales and concatenated with the dictionary of Kronecker deltas.
- **DiffusionW** (dashed purple line) [34]. These are the diffusion wavelets.
- **QMF** (solid pink line) [17]. This is the graph-QMF filter bank transform.
- **CoSubFB** (solid green line) [23]. This is the subgraph-based filter bank.

B. Approximation

Approximation is a standard task used to evaluate the quality of a representation. The goal here is to use a few expansion coefficients to approximate a graph signal. We consider two approximation strategies: nonlinear approximation and orthogonal marching pursuit. Given the budget of K expansion coefficients, nonlinear approximation chooses the K largest-magnitude ones to minimize the approximation error while orthogonal marching pursuit greedily and sequentially selects K expansion coefficients to minimize the residual error. For each representation method, we use both approximation strategies

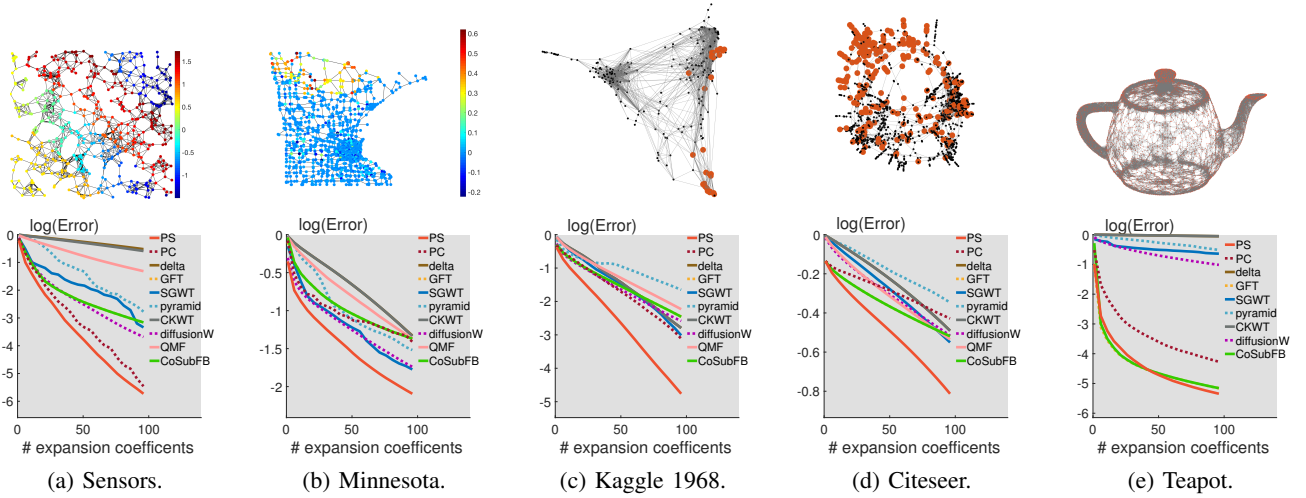


Fig. 4: Piecewise-smooth graph dictionary (in red) outperforms the other competitive methods on five datasets. The x -axis is the number of coefficients used in the approximation and the y -axis is the approximation error (5), where lower means better.

and report the results of the better one. The evaluation metric is the normalized mean square error, defined as

$$\text{Error} = \frac{\|\hat{\mathbf{x}} - \mathbf{x}\|_2^2}{\|\mathbf{x}\|_2^2}. \quad (5)$$

Figure 4 compares the approximation performances on five datasets. Five columns in Figure 4 show the sensors, Minnesota, Kaggle 1968, Citeseer and Teapot, respectively. Each plot in the first row shows the visualization of the graph signal; each plot in the second row shows the approximation error on the logarithm scale, where the x -axis is the number of expansion coefficients and the y -axis is the normalized mean square error.

Overall, the proposed piecewise-smooth graph dictionary outperforms its competitors under various types of graphs and graph signals.

- **Sensors.** The graph signal is piecewise-smooth. The top three methods are the piecewise-smooth graph dictionary, the piecewise-constant graph dictionary and the diffusion wavelets; on the other end of the spectrum, the Kronecker deltas, which fit one signal coefficient at a time, fails.

- **Minnesota.** The graph signal is localized smooth. The top three methods are the piecewise-smooth graph dictionary, the diffusion wavelets and the spectral graph wavelet transform; on the other end of the spectrum, the spatial graph wavelets fail.

- **Kaggle 1968.** The graph signal is binary and piecewise-constant with a few pieces. The top three methods are the piecewise-smooth graph dictionary, the piecewise-constant graph dictionary and the spectral graph wavelet transform; on the other end of the spectrum, the multiscale pyramid transform fails.

- **Citeseer.** The graph signal is binary, piecewise-constant with a large number of pieces. None of the methods performs well due to the noisy input signal. The top three methods are the piecewise-smooth graph dictionary, the subgraph-based filter bank and the graph-QMF filter bank transform; on the other end of the spectrum, the multiscale pyramid transform fails.

- **Teapot.** The graph signal is smooth. The top three methods are the piecewise-smooth graph dictionary, the subgraph-based filter bank and the graph Fourier basis; on the other end of the spectrum, the Kronecker deltas and the spatial graph wavelets fail. To have an illustrative understanding, we visualize the reconstructions in Figure 5 where each plot shows the reconstruction by using 100 expansion coefficients.

Additionally, Figure 6 compares the approximations of urban data supported on the Manhattan street networks. The two rows show the reconstructions of the taxi-pickup distribution and restaurant distribution, respectively, by using 100 expansion coefficients. We see that three graph signals are nonsmooth and inhomogeneous. For each of the three graph signals, the piecewise-smooth graph dictionary provides the largest signal-to-noise ratio (SNR) and smallest normalized mean square error.

The spectral graph wavelet transform is also competitive; the subgraph-based filter bank tends to be over smooth and the spatial graph wavelets tend to be less smooth.

C. Localization

One functionality of a graph dictionary is to detect localized graph signals [47]; applications include localizing virus attacks in cyber-physical systems, localizing stimuli in brain connectivity networks and mining traffic events in city street networks. We here consider simulations on the Minnesota road networks. We generate one-piece graph signals with Gaussian noises. Given the noisy graph signals, we use graph dictionary to remove noises and reconstruct a denoised graph signal to localize the underlying activated pieces. We average over 20 random trials.

Figure 7 shows the localization performance, where the x -axis is the noise level and the y -axis is either SNR or correlation. In both cases, higher value means better. The baseline (dark curve) means that we naively use the noisy graph signal as the reconstruction. We see that the piecewise-smooth graph dictionary outperforms the others in terms of both metrics,

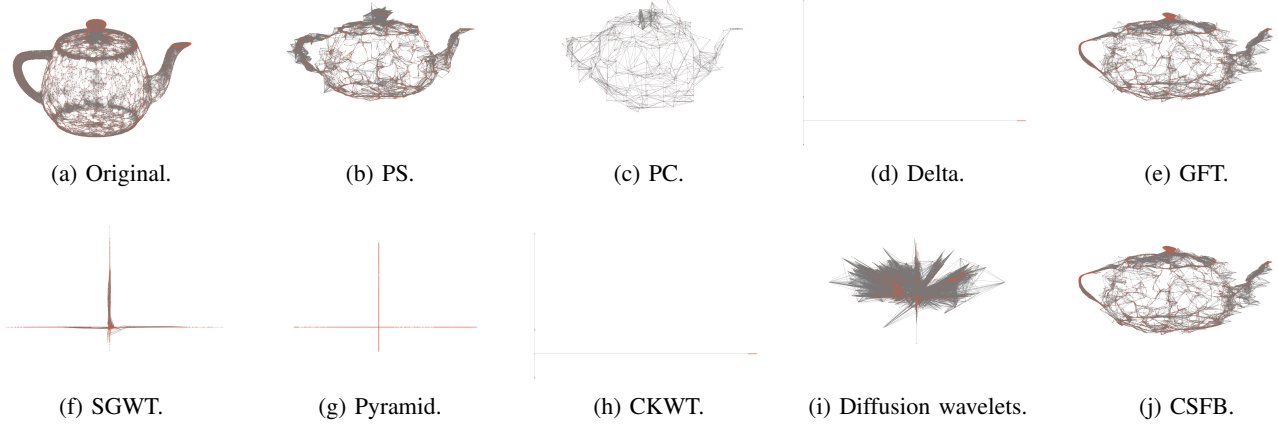


Fig. 5: Reconstruction visualization for Teapot.

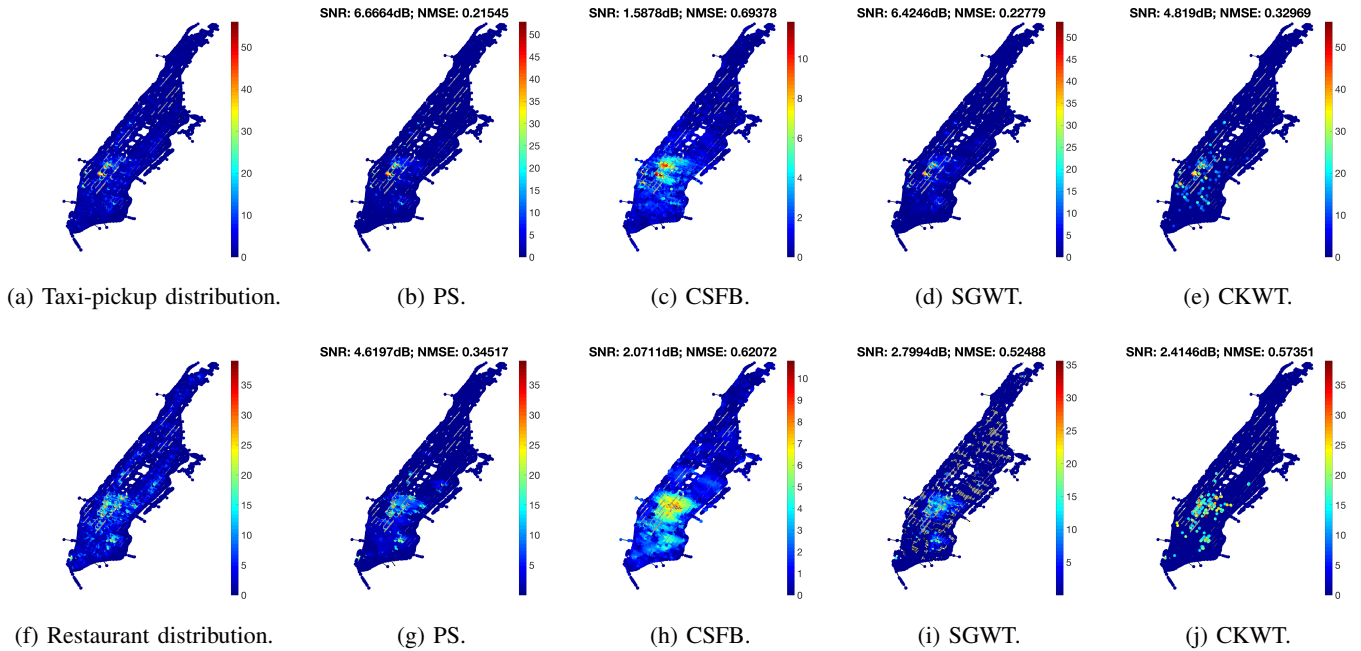


Fig. 6: Reconstruction visualization for urban data.

especially when the noise level is low; when the noise level is high, piecewise-constant graph dictionary, piecewise-smooth graph dictionary and multiscale pyramid transform perform similarly.

Figure 8 compares reconstructions. Figure 8 (a) shows the original one-piece graph signal, (b) shows the noisy graph signal, while (c), (d) and (e) show the denoised graph signals by using the piecewise-smooth graph dictionary, the subgraph-based filter bank and the spectral graph wavelet transform, respectively. We see that the piecewise-smooth graph dictionary localizes the underlying piece well, the spectral graph wavelet transform does a reasonable job, but the subgraph-based filter bank provides an over-smooth reconstruction and fails.

VII. CONCLUSIONS AND FUTURE WORKS

In this paper, we model complex and irregular data, such as urban data supported on the city street networks and profile information supported on the social networks, as piecewise-smooth graph signals. We propose a well-structured and storage-friendly graph dictionary to represent those graph signals. To ensure a good representation, we consider the graph multiresolution analysis. To implement this, we propose the coarse-to-fine approach, which iteratively partitions a graph into two subgraphs until we reach individual nodes. This approach efficiently implements the graph multiresolution analysis and the induced graph dictionary promotes sparse representations for piecewise-smooth graph signals. Finally, we test the proposed graph dictionary on the tasks of approximation and localization. The empirical results validate that the proposed graph dictionary outperforms eight other

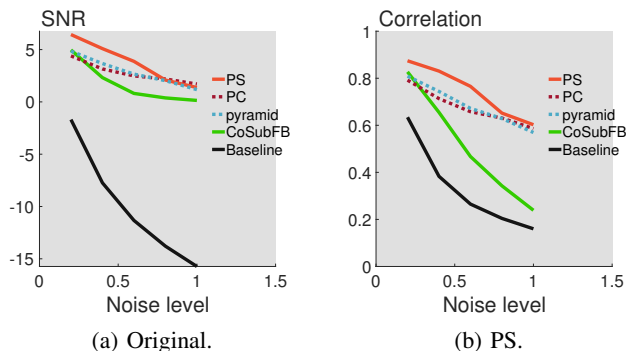


Fig. 7: Localization performance as a function of noise level. Piecewise-smooth graph dictionary (in red) outperforms the other competitive methods. The x -axis is the noise level and the y -axis is the signal-to-noise ratio (SNR), where higher means better.

representation methods on various datasets. Future works may include develop sampling, recovery, denoising and detection strategies based on the proposed piecewise-smooth graph signal model.

REFERENCES

- [1] M. Jackson, *Social and Economic Networks*, Princeton University Press, 2008.
- [2] M. Newman, *Networks: An Introduction*, Oxford University Press, 2010.
- [3] D. I. Shuman, S. K. Narang, P. Frossard, A. Ortega, and P. Vandergheynst, "The emerging field of signal processing on graphs: Extending high-dimensional data analysis to networks and other irregular domains," *IEEE Signal Process. Mag.*, vol. 30, pp. 83–98, May 2013.
- [4] A. Sandryhaila and J. M. F. Moura, "Discrete signal processing on graphs," *IEEE Trans. Signal Process.*, vol. 61, no. 7, pp. 1644–1656, Apr. 2013.
- [5] P. Prandoni and M. Vetterli, "Approximation and compression of piecewise smooth functions," *Phil. Transaction R. Soc. Lond. A.*, vol. 357, no. 1760, pp. 2573–2591, 1999.
- [6] M. B. Wakin, J. K. Romberg, H. Choi, and R. G. Baraniuk, "Wavelet-domain approximation and compression of piecewise smooth images," *IEEE Trans. Image Process.*, vol. 15, no. 5, pp. 1071–1087, 2006.
- [7] V. Chandrasekaran, M. B. Wakin, D. Baron, and R. G. Baraniuk, "Representation and compression of multidimensional piecewise functions using surflets," *IEEE Trans. Inf. Theory*, vol. 55, no. 1, pp. 374–400, 2009.
- [8] M. Unser, "Splines: A perfect fit for signal and image processing," *IEEE Signal Process. Mag.*, vol. 16, no. 6, pp. 22–38, Nov. 1999.
- [9] Y-X Wang, J. Sharpnack, A. Smola, and R. J. Tibshirani, "Trend filtering on graphs," in *AISTATS*, San Diego, CA, May 2015.
- [10] M. Vetterli, J. Kovačević, and V. K. Goyal, *Foundations of Signal Processing*, Cambridge University Press, Cambridge, 2014, <http://www.fourierandwavelets.org/>.
- [11] S. Mallat, *A Wavelet Tour of Signal Processing*, Academic Press, New York, NY, third edition, 2009.
- [12] M. Vetterli and J. Kovačević, *Wavelets and Subband Coding*, Prentice Hall, Englewood Cliffs, NJ, 1995, <http://waveletsandsubbandcoding.org/>.
- [13] M. Belkin and P. Niyogi, "Laplacian eigenmaps for dimensionality reduction and data representation," *Neur. Comput.*, vol. 13, pp. 1373–1396, 2003.
- [14] A. Sandryhaila and J. M. F. Moura, "Big data processing with signal processing on graphs," *IEEE Signal Process. Mag.*, vol. 31, no. 5, pp. 80–90, 2014.
- [15] A. Anis, A. Gadde, and A. Ortega, "Towards a sampling theorem for signals on arbitrary graphs," in *Proc. IEEE Int. Conf. Acoust., Speech, Signal Process.*, Florence, May 2014, pp. 3864–3868.
- [16] S. Chen, R. Varma, A. Sandryhaila, and J. Kovačević, "Discrete signal processing on graphs: Sampling theory," *IEEE Trans. Signal Process.*, vol. 63, no. 24, pp. 6510–6523, Dec. 2015.
- [17] S. K. Narang and A. Ortega, "Perfect reconstruction two-channel wavelet filter banks for graph structured data," *IEEE Trans. Signal Process.*, vol. 60, pp. 2786–2799, June 2012.
- [18] S. K. Narang and Antonio Ortega, "Compact support biorthogonal wavelet filterbanks for arbitrary undirected graphs," *IEEE Trans. Signal Process.*, vol. 61, no. 19, pp. 4673–4685, Oct. 2013.
- [19] V. N. Ekambaram, G. C. Fanti, B. Ayazifar, and K. Ramchandran, "Critically-sampled perfect-reconstruction spline-wavelet filterbanks for graph signals," in *GlobalSIP*, Austin, TX, Dec. 2013, pp. 475–478.
- [20] M. S. Kotzagiannidis and P. L. Dragotti, "The graph FRI framework-spline wavelet theory and sampling on circulant graphs," in *ICASSP*, Shanghai, China, Mar. 2016, pp. 6375–6379.
- [21] Y. Tanaka and A. Sakiyama, "M-channel oversampled graph filter banks," *IEEE Trans. Signal Process.*, vol. 62, no. 14, pp. 3578–3590, 2014.
- [22] D. I. Shuman, M. J. Faraji, and P. Vandergheynst, "A multiscale pyramid transform for graph signals," *IEEE Trans. Signal Process.*, vol. 64, no. 8, pp. 2119–2134, April 2016.
- [23] N. Tremblay and P. Borgnat, "Subgraph-based filterbanks for graph signals," *IEEE Trans. Signal Process.*, vol. 64, no. 15, pp. 3827–3840, August 2016.
- [24] Y. Jin and D. I. Shuman, "An m-channel critically sampled filter bank for graph signals," *Proceedings of the IEEE Conference on Acoustics, Speech, and Signal Processing*, pp. 3909–3913, March 2017.
- [25] M. Crovella and E. Kolaczyk, "Graph wavelets for spatial traffic analysis," in *Proc. IEEE INFOCOM*, Mar. 2003, vol. 3, pp. 1848–1857.
- [26] A. D. Szlam, M. Maggioni, R. R. Coifman, and J. C. Bremer Jr., "Diffusion-driven multiscale analysis on manifolds and graphs: top-down and bottom-up constructions," in *Proceedings of the SPIE, Wavelets XI*, Aug. 2005, vol. 5914, pp. 445–455.
- [27] M. Gavish, B. Nadler, and R. R. Coifman, "Multiscale wavelets on trees, graphs and high dimensional data: Theory and applications to semi supervised learning," in *Proc. Int. Conf. Mach. Learn.*, Haifa, Israel, June 2010, pp. 367–374.
- [28] R. M. Rustamov, "Average interpolating wavelets on point clouds and graphs," *CoRR*, vol. abs/1110.2227, 2011.
- [29] Jeff Irion and Naoki Saito, "Hierarchical graph laplacian eigen transforms," *SIAM Letters*, vol. 6, no. 0, pp. 21–24, Jan. 2014.
- [30] D. K. Hammond, P. Vandergheynst, and R. Gribonval, "Wavelets on graphs via spectral graph theory," *Appl. Comput. Harmon. Anal.*, vol. 30, pp. 129–150, Mar. 2011.
- [31] N. Leonardi and D. Van De Ville, "Tight wavelet frames on multislice graphs," *IEEE Trans. Signal Process.*, vol. 61, no. 13, pp. 3357–3367, 2013.
- [32] D. I. Shuman, C. Wiesmeyer, N. Holighaus, and P. Vandergheynst, "Spectrum-adapted tight graph wavelet and vertex-frequency frames," *IEEE Trans. Signal Process.*, vol. 63, no. 16, pp. 4223–4235, August 2015.
- [33] D. I. Shuman, B. Ricaud, and P. Vandergheynst, "Vertex-frequency analysis on graphs," *Applied and Computational Harmonic Analysis*, vol. 40, no. 2, pp. 260–291, March 2016.
- [34] R. R. Coifman and M. Maggioni, "Diffusion wavelets," *Appl. Comput. Harmon. Anal.*, pp. 53–94, July 2006.
- [35] J. Bremer, R. Coifman, M. Maggioni, and A. R. Szlam, "Diffusion wavelet packets," *Appl. Comput. Harmon. Anal.*, vol. 21, pp. 95–112, July 2006.
- [36] X. Zhang, X. Dong, and P. Frossard, "Learning of structured graph dictionaries," in *Proc. IEEE Int. Conf. Acoust., Speech, Signal Process.*, Kyoto, Japan, 2012, pp. 3373–3376.
- [37] D. Thanou, D. I. Shuman, and P. Frossard, "Learning parametric dictionaries for signals on graphs," *IEEE Trans. Signal Process.*, vol. 62, pp. 3849–3862, June 2014.
- [38] X. Zhu and M. Rabbat, "Approximating signals supported on graphs," in *Proc. IEEE Int. Conf. Acoust., Speech, Signal Process.*, Kyoto, Japan, Mar. 2012, pp. 3921–3924.
- [39] B. Ricaud, D. I. Shuman, and P. Vandergheynst, "On the sparsity of wavelet coefficients for signals on graphs," in *Conference on Wavelets and Sparsity XV*, 2013, vol. 8858.
- [40] W. K. Allard, G. Chen, and M. Maggioni, "Multiscale geometric methods for data sets i: Multiscale svd, noise and curvature," *Appl. Comput. Harmon. Anal.*, no. 3, pp. 504–567, 2017.
- [41] W. K. Allard, G. Chen, and M. Maggioni, "Multi-scale geometric methods for data sets ii: Geometric multi-resolution analysis," *Appl. Comput. Harmon. Anal.*, no. 3, pp. 435–462, 2012.
- [42] W. Liao and M. Maggioni, "Adaptive geometric multiscale approximations for intrinsically low-dimensional data," *arXiv preprint arXiv:1611.01179*, 2016.

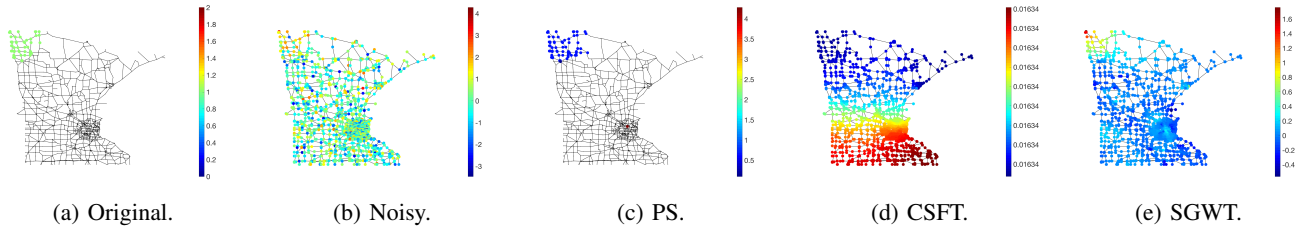


Fig. 8: Localization visualization.

- [43] U. V. Luxburg, "A tutorial on spectral clustering," *Statistics and Computing*, vol. 17, pp. 395–416, 2007.
- [44] X. Wang, P. Liu, and Y. Gu, "Local-set-based graph signal reconstruction," *IEEE Trans. Signal Process.*, vol. 63, no. 9, May 2015.
- [45] M. Tsitsvero, S. Barbarossa, and P. D. Lorenzo, "Signals on graphs: Uncertainty principle and sampling," *arXiv:1507.08822*, 2015.
- [46] G. Karypis and V. Kumar, "A fast and high quality multilevel scheme for partitioning irregular graphs," *SIAM J. Scientific Computing*, vol. 20, no. 1, pp. 359–392, 1998.
- [47] S. Chen, Y. Yang, S. Zong, A. Singh, and J. Kovačević, "Detecting localized categorical attributes on graphs," *IEEE Trans. Signal Process.*, vol. 65, pp. 2725–2740, May 2017.

APPENDIX

A. Iterated Graph Filter Bank

In this section, we generalize the classical filter banks to the graph domain and point out why the graph filter banks are hard to implement. Suppose we have an ordering of nodes $\{v_1, v_2, \dots, v_N\}$, such that two consecutive nodes v_{2k-1}, v_{2k} are connected for $k = 1, 2, \dots, K$, where $K \leq \lfloor N/2 \rfloor$. We group all pairs of v_{2k-1}, v_{2k} to form a series of connected and nonoverlapping subgraphs. The basis vectors of the k th subgraph are

$$\mathbf{v}_k^{(1)} = \frac{1}{\sqrt{2}} (\mathbf{1}_{v_{2k-1}} + \mathbf{1}_{v_{2k}}) \in \mathbb{R}^N, \quad (6)$$

$$\mathbf{u}_k^{(1)} = \frac{1}{\sqrt{2}} (\mathbf{1}_{v_{2k-1}} - \mathbf{1}_{v_{2k}}) \in \mathbb{R}^N, \quad (7)$$

where the subscript k is the index of the subgraph and the superscript 1 indicates the root layer, the low-pass basis vector $\mathbf{v}_k^{(1)}$ considers the average of two nodes within this subgraph and the high-pass basis sequence $\mathbf{u}_k^{(1)}$ considers the difference between two nodes within this subgraph. We collect all the low-pass basis vectors and high-pass basis vectors to form a low-pass subspace and a high-pass subspace, respectively,

$$V^{(1)} = \text{span} \left(\{\mathbf{v}_k^{(1)}\}_{k=1}^K \right) \text{ and } U^{(1)} = \text{span} \left(\{\mathbf{u}_k^{(1)}\}_{k=1}^K \right).$$

Different from the discrete-time scenario, $V^{(1)} \oplus U^{(1)}$ may not span the entire \mathbb{R}^N space, as a few nodes may be isolated due to the ordering. Let the residual subspace be $R^{(1)} = \text{span} \left(\{\mathbf{1}_{v_k}\}_{k=2K+1}^N \right)$, where each basis vector only activates an individual node. Now $V^{(1)} \oplus U^{(1)} \oplus R^{(1)} = \mathbb{R}^N$. For any graph signal $\mathbf{x} \in \mathbb{R}^N$, the reconstruction is

$$\mathbf{x} = \underbrace{\sum_{k=1}^K \langle \mathbf{x}, \mathbf{v}_k^{(1)} \rangle \mathbf{v}_k^{(1)}}_{\mathbf{x}_{V^{(1)}}} + \underbrace{\sum_{k=1}^K \langle \mathbf{x}, \mathbf{u}_k^{(1)} \rangle \mathbf{u}_k^{(1)}}_{\mathbf{x}_{U^{(1)}}} + \underbrace{\sum_{k=2K+1}^N \langle \mathbf{x}, \mathbf{1}_{v_k} \rangle \mathbf{1}_{v_k}}_{\mathbf{x}_{R^{(1)}}},$$

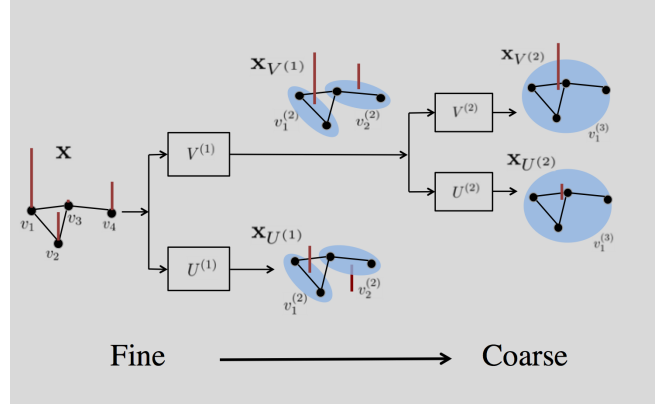


Fig. 9: As a fine-to-coarse approach, the analysis part of iterated graph filter banks implement the graph multiresolution analysis (Definition 5). There is no residual in this case.

where $\mathbf{x}_{V^{(1)}} \in V^{(1)}$ is the low-pass projection, $\mathbf{x}_{U^{(1)}} \in U^{(1)}$ is the high-pass projection and $\mathbf{x}_{R^{(1)}} \in R^{(1)}$ handles the residual condition.

To summarize, based on a well-designed ordering, we partition the entire graph into a series of nonoverlapping subgraphs and then design the Haar-like basis vectors on graphs. For discrete-time signals whose underlying graph is a directed line graph, the ordering is provided by time and each subgraph contains two consecutive time stamps. As described in Section ??, because of the nice ordering by time, all the basis vectors can be efficiently obtained by filtering following by downsampling; however, this is not true for arbitrary graphs.

Following the classical discrete-time signal processing, we can iteratively decompose the low-pass subspace and obtain smoother and smoother subspaces, which is equivalent to coarsen in the graph vertex domain. This iterated graph filter bank divides the vertex-spectrum plane into more tiles, approaching to the limit of uncertainty barrier. Here we show the second layer for an example. Let a supernode (connected node set) $v_k^{(2)} = v_{2k-1} \cup v_{2k}$ for $k = 1, 2, \dots, K$, where the superscript of the supernode indicates the second layer. Two supernodes $v_i^{(2)}, v_j^{(2)}$ are connected when there exists a pair of nodes $p \in v_i^{(2)}, q \in v_j^{(2)}$ satisfying that p, q are connected. Similarly to the paradigm in Section A, suppose we have an ordering of K supernodes $\{v_1^{(2)}, v_2^{(2)}, \dots, v_K^{(2)}\}$, such that two consecutive supernodes $v_{2k-1}^{(2)}, v_{2k}^{(2)}$ are connected for $k = 1, \dots, K^{(2)}$, where $K^{(2)} \leq \lfloor K/2 \rfloor$. We group all $v_{2k-1}^{(2)}, v_{2k}^{(2)}$ to form a series of connected, yet nonoverlapping

subgraphs. Let $S_1, S_2 \subset \mathcal{V}$ be two nonoverlapping supernodes. We define the low-pass and high-pass Haar template basis vector are, respectively,

$$g(S_1, S_2) = \sqrt{\frac{|S_1||S_2|}{|S_1|+|S_2|}} \left(\frac{\mathbf{1}_{S_1}}{|S_1|} + \frac{\mathbf{1}_{S_2}}{|S_2|} \right) \in \mathbb{R}^N,$$

$$h(S_1, S_2) = \sqrt{\frac{|S_1||S_2|}{|S_1|+|S_2|}} \left(\frac{\mathbf{1}_{S_1}}{|S_1|} - \frac{\mathbf{1}_{S_2}}{|S_2|} \right) \in \mathbb{R}^N.$$

Following from the template, the basis vectors of the k th subgraph are

$$\begin{aligned} \mathbf{v}_k^{(2)} &= g(v_{2k-1}^{(2)}, v_{2k}^{(2)}), \\ \mathbf{u}_k^{(2)} &= h(v_{2k-1}^{(2)}, v_{2k}^{(2)}). \end{aligned}$$

We collect all the low-pass basis vectors and high-pass basis vectors in the second layer to form a low-pass subspace and a high-pass subspace, respectively,

$$V^{(2)} = \text{span} \left(\{ \mathbf{v}_k^{(2)} \}_{k=1}^{K^{(2)}} \right) \text{ and } U^{(2)} = \text{span} \left(\{ \mathbf{u}_k^{(2)} \}_{k=1}^{K^{(2)}} \right).$$

Let the residual subspace be $R^{(2)} = \text{span} \left(\{ \mathbf{1}_{v_n^{(2)}} \}_{n=2K^{(2)}+1}^K \right)$, where each basis vector only activates an individual supernode. Now $V^{(2)} \oplus U^{(2)} \oplus R^{(2)} = V^{(1)}$.

For any graph signal $\mathbf{x} \in \mathbb{R}^N$, the reconstruction is

$$\begin{aligned} \mathbf{x} &= \underbrace{\sum_{k=1}^{K^{(2)}} \langle \mathbf{x}, \mathbf{v}_k^{(2)} \rangle \mathbf{v}_k^{(2)}}_{\in V^{(2)}} + \underbrace{\sum_{k=1}^{K^{(2)}} \langle \mathbf{x}, \mathbf{u}_k^{(2)} \rangle \mathbf{u}_k^{(2)}}_{\in U^{(2)}} + \underbrace{\sum_{k=1}^K \langle \mathbf{x}, \mathbf{u}_k^{(1)} \rangle \mathbf{u}_k^{(1)}}_{\in U^{(1)}} \\ &+ \underbrace{\sum_{k=2K+1}^N \langle \mathbf{x}, \mathbf{1}_{v_k} \rangle \mathbf{1}_{v_k}}_{\in R^{(1)}} + \underbrace{\sum_{k=2K^{(2)}+1}^K \langle \mathbf{x}, \mathbf{1}_{v_k^{(2)}} \rangle \mathbf{1}_{v_k^{(2)}}}_{\in R^{(2)}}. \end{aligned}$$

We can keep decomposing the low-pass subspace until there is only one constant basis vector. During the iterated decomposition, we keep coarsening in the graph vertex domain, leading to larger supernodes and more global-wise basis vectors; we thus call this a *fine-to-coarse approach*; see Figure 9.

Let the decomposition depth be L . By induction, the general reconstruction is

$$\begin{aligned} \mathbf{x} &= \underbrace{\sum_{k=1}^{K^{(L)}} \langle \mathbf{x}, \mathbf{v}_k^{(L)} \rangle \mathbf{v}_k^{(L)}}_{\in V^{(L)}} + \underbrace{\sum_{\ell=1}^L \sum_{k=1}^{K^{(\ell)}} \langle \mathbf{x}, \mathbf{u}_k^{(\ell)} \rangle \mathbf{u}_k^{(\ell)}}_{\in U^{(\ell)}} \\ &+ \underbrace{\sum_{\ell=1}^L \sum_{k=2K^{(\ell)}+1}^{K^{(\ell-1)}} \langle \mathbf{x}, \mathbf{1}_{v_k^{(\ell)}} \rangle \mathbf{1}_{v_k^{(\ell)}}}_{\in R^{(\ell)}}, \end{aligned}$$

where $v_k^{(1)} = v_k$, $K^1 = K$ and $K^0 = N$.

Note that for discrete-time signals, the ordering of time stamps is naturally provided by time, leading to straightforward downsampling and shifting, and iterated filter banks, as a fine-to-coarse approach, are efficient architectures to implement the multiresolution analysis. For graph signals, the ordering in each multiresolution level is unknown and an efficient fine-to-coarse approach to implement the graph multiresolution analysis is not

straightforward any more. This is why we consider the coarse-to-fine approach in this paper; in other words, we convert the problem of node ordering to the problem of graph partitioning, which is more efficient and straightforward.

B. Proof of Theorem 1

Proof. First, we show each vector has norm one.

$$\begin{aligned} &\left\| \sqrt{\frac{|S_1||S_2|}{|S_1|+|S_2|}} \left(\frac{1}{|S_1|} \mathbf{1}_{S_1} - \frac{1}{|S_2|} \mathbf{1}_{S_2} \right) \right\|_2^2 \\ &\stackrel{(a)}{=} \left\| \sqrt{\frac{|S_1||S_2|}{|S_1|+|S_2|}} \frac{\mathbf{1}_{S_1}}{|S_1|} \right\|_2^2 + \left\| \sqrt{\frac{|S_1||S_2|}{|S_1|+|S_2|}} \frac{\mathbf{1}_{S_2}}{|S_2|} \right\|_2^2 \\ &= 1, \end{aligned}$$

where (a) follows from that $S_1 \cap S_2 = \emptyset$. Second, we show each vector is orthogonal to the other vectors. We have

$$\mathbf{1}^T \mathbf{w} = \sqrt{\frac{|S_1||S_2|}{|S_1|+|S_2|}} \left(\sum_{i \in S_1} \frac{1}{|S_1|} - \sum_{i \in S_2} \frac{1}{|S_2|} \right) = 0.$$

Thus, each vector is orthogonal to the first vector, $\mathbf{1}_{\mathcal{V}}/\sqrt{|\mathcal{V}|}$. Each other individual vector is generated from two node sets. Let S_1, S_2 generate \mathbf{w}_i and S_3, S_4 generate \mathbf{w}_j . Due to the construction, there are only two conditions, two node sets of one vector belong to one node set of the other vector, and all four node sets do not share element with each other. For the first case, without losing generality, let $(S_3 \cup S_4) \cap S_1 = S_3 \cup S_4$, we have

$$\begin{aligned} &\mathbf{w}_i^T \mathbf{w}_j \\ &= \sqrt{\frac{|S_1||S_2|}{|S_1|+|S_2|} \frac{|S_3||S_4|}{|S_3|+|S_4|}} \left(\sum_{i \in S_3} \frac{1}{|S_3|} - \sum_{i \in S_4} \frac{1}{|S_4|} \right) \\ &= 0. \end{aligned}$$

For the second case, the inner product between \mathbf{w}_i and \mathbf{w}_j is zero because their supports do not match. Third, we show that \mathbf{W} spans \mathbb{R}^N . Since we recursively partition the node set until the cardinalities of all the node sets are smaller than 2, there are N vectors in \mathbf{W} . \square

C. Proof of Theorem 2

Proof. We first show that $\mathcal{V}_1, \mathcal{V}_2$ are connected and then bound the cardinality difference. Since the original graph is connected, D_{v_i, v_j} is finite, where v_i, v_j are two hubs. In Step 4, we partition the nodes according to their distances to two hubs. Every node in the node set S_1 is connected to v_j ; thus, the subgraph induced by the node set S_1 is connected. In Step 5, we partition the boundary set S_2 into connected node sets, C_1, C_2, \dots, C_M , and each of them connects to S_1 ; otherwise, the maximum element in the geodesic distance matrix D is infinity. We thus have $S_1 \cup C_1 \cup C_2 \dots \cup C_m$ is connected for all $m = 1, \dots, M$. When we set $m = m^*$ obtained in Step 7, we have $\mathcal{V}_1 = S_1 \cup C_1 \cup C_2 \dots \cup C_{m^*}$ is connected. Similarly, we can show that \mathcal{V}_2 is also connected.

In Step 3, we set p as the median value of the differences to two hubs, which sets $|S_1|$ around $|\mathcal{V}_0|/2$. In Step 6, we sequentially add connected components to S_1 and finally choose the

one, whose cardinality is closest to $|\mathcal{V}_0|/2$. The last component added to S_1 is C_{m^*} , which ensures that $||\mathcal{V}_1| - |\mathcal{V}_0|/2| \leq |C_{m^*}|$ and $||\mathcal{V}_2| - |\mathcal{V}_0|/2| \leq |C_{m^*}|$. \square

D. Proof of Theorem 3

Proof. When an edge $e \in \text{supp}(\Delta \mathbf{w})$, where \mathbf{w} is one basis vector in the graph wavelet basis W , Δ is the graph incident matrix, and supp denotes the edge indices activated by the nonzero elements of $\Delta \mathbf{w}$; we call that the edge e is activated by the wavelet basis vector \mathbf{w} . Since in each level, the pieces are disjoint, each edge will be activated at most once in each level; in total, each edge will be activated by at most L wavelet basis vectors, where L the decomposition level. Let $\text{activations}(e)$ be the number of wavelet basis vectors in W that activates e .

$$\begin{aligned} \|W^T \mathbf{x}\|_0 &\leq 1 + \sum_{e \in \text{Supp}(\Delta \mathbf{w})} \text{activations}(e) \\ &\leq 1 + \|\Delta \mathbf{x}\|_0 L, \end{aligned}$$

where 1 comes from the activation of the first column vector, which is constant. Since we promote the bisection scheme, the decomposition level L is roughly $1 + \log_2 N$. \square

E. Proof of Theorem 4

Proof. The main idea is that we approximate a bandlimited signal in the original graph by using bandlimited signals in subgraphs. Based on the eigenvectors of graph Laplacian matrix, we define the bandlimited space, where each signal can be represented as $\mathbf{x} = V_{(K)} \mathbf{a}$, where $V_{(K)}$ is the submatrix of V containing the first K columns in V . We can show that this bandlimited space is a subspace of the small-variation space $\{\mathbf{x} : \mathbf{x}^T L \mathbf{x} \leq \lambda_K \mathbf{x}^T \mathbf{x}\}$.

$$\begin{aligned} \mathbf{x}^T L \mathbf{x} &= \sum_{i,j \in \mathcal{E}} W_{i,j} (x_i - x_j)^2 \\ &= \sum_{S_c} \sum_{i,j \in \mathcal{E}_{S_c}} W_{i,j} (x_i - x_j)^2 + \sum_{i,j \in (\mathcal{E} \setminus \cup_c \mathcal{E}_{S_c})} W_{i,j} (x_i - x_j)^2 \\ &= \sum_{S_c} \mathbf{x}_{S_c}^T L_{S_c} \mathbf{x}_{S_c} + \mathbf{x}^T L_{\text{cut}} \mathbf{x} \leq \lambda_K \mathbf{x}^T \mathbf{x}, \end{aligned}$$

where L_{S_c} is the graph Laplacian matrix of the subgraph G_{S_c} and L_{S_c} stores the residual edges, which are cut in the graph partition algorithm.

Thus, $\{\mathbf{x} : \mathbf{x}^T L \mathbf{x} \leq \lambda_K \mathbf{x}^T \mathbf{x}\}$ is a subset of $\bigcup_{S_c} \{\mathbf{x}_{S_c} : \mathbf{x}_{S_c}^T L_{S_c} \mathbf{x}_{S_c} \leq \lambda_K \mathbf{x}^T \mathbf{x} - \mathbf{x}^T L_{\text{cut}} \mathbf{x}\}$; that is, any small-variation graph signal in the whole graph can be precisely represented by small-variation graph signals in the subgraphs.

In each local set, when we use the bandlimited space $\{\mathbf{x} : \mathbf{x} = V_{S_c(K)} \mathbf{a}\}$ to approximate the space $\{\mathbf{x}_{S_c} : \mathbf{x}_{S_c}^T L_{S_c} \mathbf{x}_{S_c} \leq c \mathbf{x}_{S_c}^T \mathbf{x}_{S_c}\}$, the maximum error we suffer from is $c \mathbf{x}_{S_c}^T \mathbf{x}_{S_c} / \lambda_{K+1}^{(S_c)}$, which is solved by the following optimization problem,

$$\begin{aligned} \max_{\mathbf{x}} & \|\mathbf{x} - V_{S_c} V_{S_c}^T \mathbf{x}\|_2^2 \\ \text{subject to} & : \mathbf{x}^T L_{S_c} \mathbf{x} \leq c \mathbf{x}^T \mathbf{x}. \end{aligned}$$

In other words, in each local set, the maximum error to represent $\{\mathbf{x}_{S_c} : \mathbf{x}_{S_c}^T L_{S_c} \mathbf{x}_{S_c} \leq \lambda_K \mathbf{x}^T \mathbf{x} - \mathbf{x}^T L_{\text{cut}} \mathbf{x}\}$ is

$(\lambda_K \mathbf{x}^T \mathbf{x} - \mathbf{x}^T L_{\text{cut}} \mathbf{x}) / \lambda_{K+1}^{(S_c)}$. Since all the local sets share the variation budget of $\lambda_K \mathbf{x}^T \mathbf{x}$ together, the maximum error we suffer from is

$$\epsilon_{\text{par}} = \frac{\mathbf{x}^T (\lambda_K I - L_{\text{cut}}) \mathbf{x}}{\min_{S_c} \lambda_{K+1}^{(S_c)} \|\mathbf{x}\|_2^2},$$

which depends on the property of graph partitioning.

In Corollary 1, we have shown that we need at most $2L \|\Delta \mathbf{x}_{\text{PC}}\|_0$ local sets to represent the piecewise-constant template of \mathbf{x} . Since we use at most K eigenvectors in each local set, we obtain the results in Theorem 4. \square